

SOLVING PERIODIC EIGENPROBLEMS BY SOLVING CORRESPONDING EXCITATION PROBLEMS IN THE DOMAIN OF THE EIGENVALUE

T. F. Eibert^{*}, Y. Weitsch, H. Chen, and M. E. Gruber

Technische Universität München, Lehrstuhl für Hochfrequenztechnik,
Munich 80290, Germany

Abstract—Periodic eigenproblems describing the dispersion behavior of periodically loaded waveguiding structures are considered as resonating systems. In analogy to resonators, their eigenvalues and eigensolutions are determined by solving corresponding excitation problems directly in the domain of the eigenvalue. Arbitrary excitations can be chosen in order to excite the desired modal solutions, where in particular lumped ports and volumetric current distributions are considered. The method is employed together with a doubly periodic hybrid finite element boundary integral technique, which is able to consider complex propagation constants in the periodic boundary conditions and the Green's functions. Other numerical solvers such as commercial simulation packages can also be employed with the proposed procedure, where complex propagation constants are typically not directly supported. However, for propagating waves with relatively small attenuation, it is shown that the attenuation constant can be determined by perturbation methods. Numerical results for composite right/left-handed waveguides and for the leaky modes of a grounded dielectric slab are presented.

1. INTRODUCTION

Linear systems are well characterized by their eigenvalues and eigensolutions. With this knowledge, it is possible to determine the solutions of the corresponding driven problems just by a projection of the excitation onto the eigensolutions. For many problems such as waveguides and resonators, the eigensolutions are of direct importance and their knowledge is required to characterize the performance of

Received 24 January 2012, Accepted 17 February 2012, Scheduled 8 March 2012

* Corresponding author: Thomas F. Eibert (eibert@tum.de).

these devices. Therefore, the solution of eigenproblems has always been of great interest. Basically, any electromagnetic field problem formulation can be considered as an eigenproblem (without excitation) and almost any numerical solver for electromagnetic field problems offers a specific eigenproblem solver. These numerical eigenproblem solvers cast the field problem in form of a linear equation system, for which the eigenvalues and eigensolutions are to be found. An overview of solution methods for such numerical eigenproblems is given in [1, 2] and even specialized software packages with a collection of advanced methods are available, e.g., see [3].

For large numerical systems, the solution of the eigenproblems is often much more demanding than the solution of the corresponding driven problems and the convergence behavior is often not satisfying. Many electromagnetic field problems even lead to nonlinear eigenproblems (e.g., integral equation formulations where the system matrix depends in a complicated form on the eigenvalue, problems with perfectly matched layers, etc.), of which the solution is even more challenging. Many eigenproblem computations in electromagnetics are therefore restricted to relatively small problem sizes as found in the analysis of the dispersion behavior of waveguides, where it is sufficient to solve a two-dimensional eigenproblem. Another important application area for eigenproblem solutions are periodic configurations in one, two or three dimensions. Such problems have gained considerable interest over the past years, in particular in connection with the design and understanding of artificial materials composed of periodically repeated unit cells. In a numerical solution, these periodic problems require often more discretization unknowns than two-dimensional discretizations of uniform cylindrical waveguides and the resulting eigenproblems can have a considerable number of unknowns.

One way to achieve a more reliable and efficient solution of large eigenproblems for dispersion analysis of periodic configurations is a reduction of the number of unknowns by expanding the fields in the periodic boundaries in form of modal series, where the modes are typically eigenmodes of the homogeneous host waveguide or material, e.g., see [4–6]. Based on this expansion, the S -parameters and subsequently the T -parameters are obtained from driven simulations and the periodic eigenproblem is finally formulated with the typically very small number of T -parameters. This procedure is very useful, if it is possible to describe the problem with a small number of port modes. For complicated field distributions in the periodic boundaries or for open problems, the method is problematic and not straightforward.

Another way to simplify the eigenproblem is given by the so-called Trefftz method [7, 8], where particular solutions of the governing

differential equation are employed to derive a boundary integral formulation of the problem. Thus, the resulting number of unknowns is often very small, but the method is restricted to homogeneous or at least piece-wise homogeneous solution domains and particular solutions of the governing differential equation must be available. A particular Trefftz method is the so-called method of fundamental solutions [9, 10], where the particular solutions are generated by placing sources outside of the considered solution domain.

In [10–12], so-called methods of external and internal excitation are proposed for the solution of eigenproblems. These methods apply an excitation to the eigenproblem under consideration and observe a norm of the solution dependent on the varying eigenvalue. The maxima of the norm indicate the sought eigenvalues. The method is implemented together with two different regularization schemes. In [10, 11] homogeneous waveguide problems and in [12] generalized Sturm-Liouville problems are considered. The particular property of these methods is that they do not require the solution of an algebraic eigenproblem, but the repeated solution of corresponding excitation problems.

Inspired from the analogy of resonators and eigenproblems [13–15], we pursue a similar strategy which can be seen as a method of internal excitation and employ it for dispersion analysis of periodic waveguiding configurations. By a careful design of the applied excitations, e.g., by ports which are appropriately coupled to the field problem, circuit related considerations are possible and can be used for problem regularization as well as energy and power considerations. By distributed current densities, e.g., a few different distributions covering the whole solution domain, or by employing electric and magnetic excitation current densities, it is possible to guarantee that any possible mode is excited.

The approach is implemented in a hybrid finite element boundary integral (FEBI) solver for doubly periodic structures, which is well-suited for one- and two-dimensional artificial material compositions [16, 17]. This solver works with an edge-based periodic boundary condition (PBC) in the FE part of the code, whereas a spectral domain integral equation with a Floquet mode based periodic Green's function is used. Due to the BI, this solver is able to fully account for open problems. Also, lossy materials can be considered. This solver was upgraded to support complex propagation constants within its PBC and the Green's functions. Alternatively, the proposed procedure can be employed together with other numerical electromagnetics solvers, where in particular CST MWS [18] is considered in this work. Since such solvers are typically not able

to directly support complex propagation constants, a perturbation technique is presented, which is useful for the determination of relatively small attenuation constants of propagating waves. Since the proposed method requires the repeated solution of excitation problems for slightly varying parameters, start vector estimation methods based on previous solutions together with effective eigenvalue search techniques are employed in order to achieve fast convergence.

It should be noted that the treatment of eigenproblems as excitation problems has been known for a long time. However, common techniques such as those discussed in [19] or [20] or even the so-called singularity expansion method [21] excite the eigenproblem in the time domain and try to extract all eigenvalues (eigenfrequencies) from the time domain observation. Such methods can never focus the entire excitation energy into an isolated eigenfrequency and they are restricted by the always limited observation time, where even several eigenmodes have to be resolved simultaneously. In contrast, our method and the methods presented in [11, 12] directly work in the domain of the eigenvalue and have thus the possibility to direct the entire excitation energy into one isolated eigenmode. Moreover, not only eigenfrequencies are considered in this paper, but also complex propagation constants. By adaptive regularization, it is possible to focus on the individual eigenvalues, where even complex eigenvalues result in arbitrarily narrow resonance singularities.

2. PERIODIC EIGENPROBLEM FORMULATION

Consider a periodic eigenproblem in form of an operator equation

$$\mathcal{L}(\omega, \mathbf{k}_0) \{\mathbf{x}\} = 0 \quad (1)$$

with suppressed time dependence $e^{j\omega t}$ and the three-dimensional (3D) wave vector \mathbf{k}_0 defining the non-periodic functional dependence in space according to Floquet's theorem. The operator $\mathcal{L}\{\cdot\}$ represents some form of Maxwell's equations together with appropriate boundary conditions as well as material relations. \mathbf{x} is the vector solution of the operator equation. The boundary conditions can be periodic in one, two or three dimensions and they can be combined with other boundary conditions such as perfect electric conductor (PEC), perfect magnetic conductor (PMC) or absorbing boundary condition (ABC). The ABCs are often realized in form of a perfectly matched layer (PML) or a BI and they typically lead to nonlinear eigenproblems.

The eigenvalues to be found are pairs of (ω, \mathbf{k}_0) , which render the operator singular (null space of the operator). Various pairs of (ω, \mathbf{k}_0) eventually form the dispersion relation of the periodic material. For every pair of (ω, \mathbf{k}_0) one or more eigensolutions \mathbf{x} can be found.

In numerical solutions, the operator equation is typically discretized (e.g., by FE or finite difference (FD) methods, by method of moments (MoM) solutions of integral equations, or by hybrid methods) resulting in a linear equation system

$$[A_{mn}(\omega, \mathbf{k}_0)] \{x_n\} = 0, \quad (2)$$

which must become singular. x_n are the unknown expansion coefficients of the field solution and A_{mn} are the matrix entries (row m , column n) depending on (ω, \mathbf{k}_0) . Numerical methods for solution of eigenproblems in linear equation form are found in [1–3], where these methods typically focus on linear eigenproblems in standard form.

3. EIGENPROBLEM-RESONATOR EQUIVALENCE AND EXCITATION FORMULATION

In the field of electric circuits, the basic shunt resonator consisting of a capacitor C and an inductor L together with a loss conductance G_l is an example for an eigenproblem. The eigenvalue is the resonance frequency ω_{res} of the resonator (excluding load and generator), for which the equation

$$Y(\omega)U = \left[j \left(\omega C - \frac{1}{\omega L} \right) + G_l \right] U = 0 \quad (3)$$

becomes singular. For lossy resonators, ω_{res} will be a complex quantity, which becomes real for vanishing G_l .

In the case of circuits, it is quite common to analyze the resonance behavior of resonators by applying an excitation and by observing the reaction (voltage) to the excitation. This procedure is physically intuitive and can be realized by measurements. Also, the generator and load resistors can be used to regularize the singular resonance behavior without leading to a shift of the resonance frequency as long as the original field problem is not modified.

In the following, similar procedures are employed for the solution of eigenproblems according to (1). The eigenproblem will be considered as some kind of a virtual resonator as illustrated in Fig. 1(a). In many cases, it will be possible to excite the field problem with ports, but other ways of excitation such as impressed current densities somewhere in the solution domain are also possible. Also, it is not necessarily required to observe the voltage across the port resistors. It is rather possible to work with some arbitrary observable of the field solution such as the electric field within the solution domain or some integral measure of it (as for instance suggested in [11,12]). A particular strength of this method is that the excitation can be chosen in a

way that a desired eigenmode is more excited than others. Also, with appropriately chosen volumetric sources (e.g., volume current density with randomly changing amplitude and phase throughout the whole solution domain) it is possible to excite all relevant eigenmodes. Assuming electric and magnetic excitation current densities, it is clear that every mode can be excited since electric and magnetic fields of one mode are never exactly zero at identical locations.

If it is feasible to connect a pair of ports to the eigenproblem as shown in Fig. 1(a), it is often directly possible to find the resonances directly from the port S -parameters. Dependent on the eigenproblem configuration, it may, however, happen that the coupling of the ports to the field problem introduces a reactive coupling element (capacitive or inductive) as indicated in Fig. 1(a). This coupling element does influence the resonance curve of the S -parameters, but other observables such as the fields in the solution domain will still directly indicate the resonance and by this the eigenvalue.

Once the eigenvalue (or the resonance) is found, the energy balance of the problem can be evaluated in order to perform a power loss analysis in the form of a perturbation technique [14, 22]. The transported power through the unit cell can be computed from the eigensolution, the field solution in the unit cell, by integrating the power flow over the waveguide cross section. The power loss can be

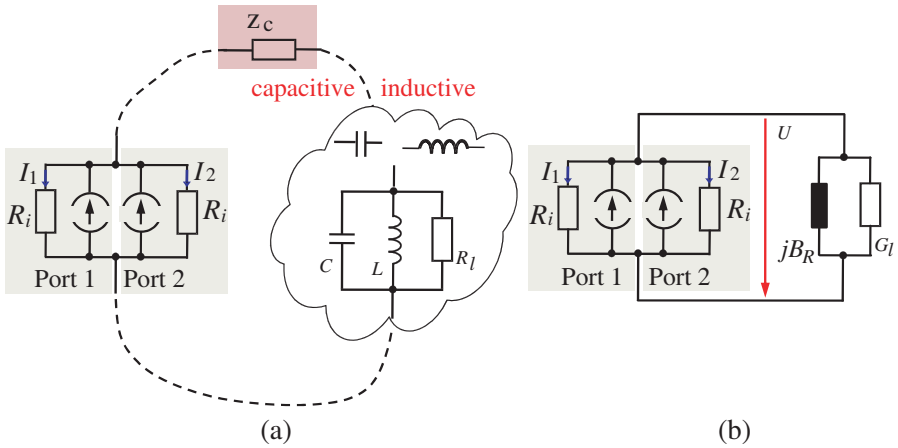


Figure 1. Excitation of general eigenproblem by ports according to circuit equivalence. Dependent on the configuration, a parasitic reactive coupling element can be present. The port voltage applies always to the shunt resistor of the resonator (see (b)). (a) Equivalent circuit. (b) Circuit at resonance.

considered as the power loss in the conductance G_l in the equivalent circuit in Fig. 1(b), which is determined at resonance. In more general cases, where the circuit based consideration is not feasible, the power loss can be computed by integrating the power loss density in the solution volume and the power flow through the non-periodic boundaries.

In summary, the proposed solution procedure is as follows: A dispersion or eigenproblem according to (1) or (2) is solved by exciting the problem in some way and monitoring an observable quantity. The eigenvalues are found where the observable assumes a maximum. These eigenvalues are pairs of (ω, \mathbf{k}_0) . In the realization, it is possible to fix \mathbf{k}_0 and vary ω until the maximum of the observable is found. In the case of propagating modes, it is then possible to determine their attenuation constant in a perturbation sense [14, 22].

A second possibility is to fix ω and vary \mathbf{k}_0 until the maximum of the observable is found. This makes it even possible to search for complex \mathbf{k}_0 and thus for propagating modes with strong attenuation, for evanescent modes or for leaky modes.

The modal field solution is directly obtained together with the eigenvalue. For degenerate modes it is, however, necessary to solve the problem with different excitations and perform an orthogonalization of the modal field solutions.

In the next section, a hybrid FEBI method for 2D periodic problems will be discussed, which has been upgraded for consideration of complex \mathbf{k}_0 . However, other numerical implementations such as commercial software packages may be used, where typically complex \mathbf{k}_0 cannot be imposed via the PBC. In this case, it is however still possible to utilize the discussed perturbation technique.

4. HYBRID FINITE ELEMENT BOUNDARY INTEGRAL (FEBI) METHOD FOR 2D PERIODIC PROBLEMS

Consider a geometric configuration as illustrated in Fig. 2. The geometric material distribution is doubly periodic in the xy -plane with lattice vectors $\boldsymbol{\rho}_a$ and $\boldsymbol{\rho}_b$. The possibly inhomogeneous parts are contained in one layer, which is represented by the indicated unit cell discretized by a tetrahedral FE mesh. Below and above the possibly inhomogeneous layer, there might be an arbitrary number of homogeneous cover layers, which can of course be considered as periodic with the lattice vectors $\boldsymbol{\rho}_a$ and $\boldsymbol{\rho}_b$, too. Employing the Floquet theorem, we factor the field solution in the structure according to

$$\mathbf{E}(\mathbf{r} + m\boldsymbol{\rho}_a + n\boldsymbol{\rho}_b) = \mathbf{E}(\mathbf{r})e^{-j\mathbf{k}_{t00} \cdot (m\boldsymbol{\rho}_a + n\boldsymbol{\rho}_b)} \quad (4)$$

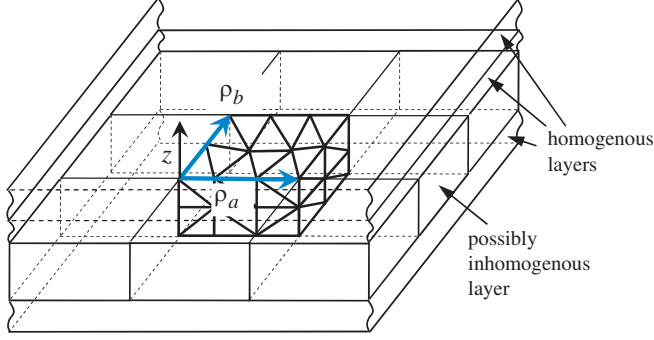


Figure 2. 2D infinite periodic configuration.

into a periodic and a non-periodic part. \mathbf{k}_{t00} corresponds to \mathbf{k}_0 in (1), where the subscript $t00$ indicates that the wavevector is in parallel to the xy -plane and the (00) th Floquet mode with respect to the 2D Floquet mode series. The field problem is modeled by a FE/BI method, of which details are found in [16]. According to the Floquet theorem, only the tetrahedral unit cell mesh is considered within the FE technique. For the present work, it is important that the PBCs have been implemented for arbitrary complex \mathbf{k}_{t00} , i.e., under consideration of attenuation. In the BI employed on the planar top and bottom surfaces of the FE unit cell mesh, the appropriate spectral domain 2D periodic Green's functions including the influence of the homogeneous material layers below and above the FE unit cell mesh are used [17]. For free space above and below the unit cell, the scalar half-space Green's function of the Helmholtz equation in form of

$$G(\mathbf{r}, \mathbf{r}') = \sum_{m=-\infty}^{+\infty} \sum_{n=-\infty}^{+\infty} \frac{e^{-j\mathbf{k}_{tmn} \cdot (\boldsymbol{\rho} - \boldsymbol{\rho}')}}{2Ajk_{zmn}} e^{-jk_{zmn}|z-z'|} \quad (5)$$

with $\mathbf{r} = \boldsymbol{\rho} + z\hat{z}$, $A = |\boldsymbol{\rho}_a \times \boldsymbol{\rho}_b|$ and

$$k_{zmn} = \pm \sqrt{k_0^2 - \mathbf{k}_{tmn} \cdot \mathbf{k}_{tmn}} \quad (6)$$

$$\mathbf{k}_{tmn} = \mathbf{k}_{t00} + \frac{2\pi}{A} [n(\hat{z} \times \boldsymbol{\rho}_a) + m(\boldsymbol{\rho}_b \times \hat{z})] \quad (7)$$

can be used, where the infinite Floquet mode series can be typically terminated after a few terms. Again it is important, that the Green's functions are implemented in a way that complex \mathbf{k}_{t00} are possible. With $k_0 = \omega \sqrt{\mu_0 \varepsilon_0}$ (i.e., the free-space wavenumber) it is obvious that the BI representation (realizing an open boundary condition) leads to a nonlinear eigenproblem.

Important is the correct choice of the sign of the square root in (6), in particular for complex modes as of interest in this paper. The situation is illustrated in Fig. 3 in the complex transverse wavenumber plane of k_y (assuming $k_x = 0$) for a waveguiding structure, which is closed at its lower end of z but open for large z . Appropriate branch cuts according to [23] have been chosen in a way that the complete upper Riemann sheet represents proper modes. Real Floquet modes are interpreted and illustrated as discrete samples along the Sommerfeld integration path as employed for non-periodic configurations. If complex Floquet modes with attenuation in power flow direction are considered, $\Im(k_y)$ becomes negative as shown in the figure. The complex Floquet modes are now considered as discrete samples of a locally deformed Sommerfeld integration path (deformation only at the position of the Floquet mode samples as indicated by the arrows in the figure). It is obvious that all complex modes remain proper (on the top Riemann sheet) except for modes, which are located between the origin and the branch point k (typically

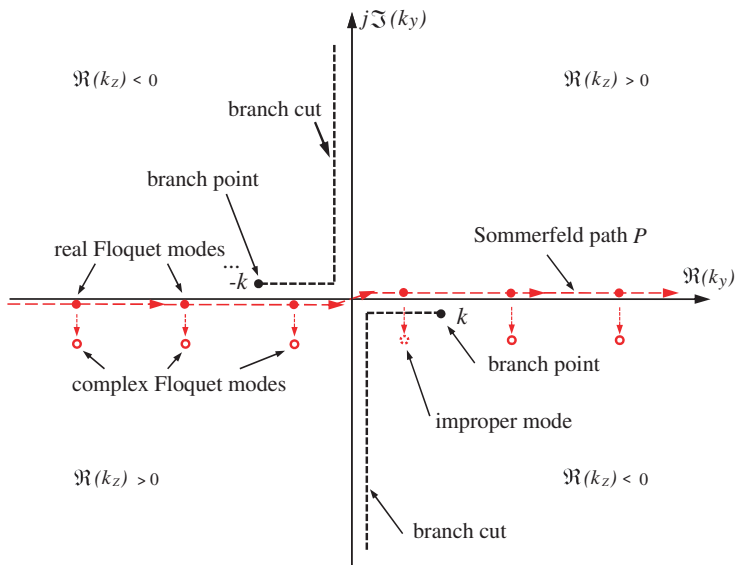


Figure 3. Illustration of real and complex Floquet modes in the complex transverse wavenumber plane of k_y , where k_x is assumed 0, for a waveguiding structure, which is closed at its lower end of z but open for large z . The branch cut definition is according to [23] and the classical Sommerfeld integration path for non-periodic problems is also given. Shown is the proper Riemann sheet, where $\Im(k_z) < 0$.

$k = k_0$ for free space corresponding to the material in the halfspace above the configuration). These modes cross the branch cut as required by a regular deformation of the Sommerfeld integration path and move onto the lower improper Riemann sheet. This is, however, in agreement with what is expected. Radiating right-handed leaky modes are known to be improper, whereas left-handed leaky modes are proper.

In order to realize the eigenproblem computation as described in Section 3, volume current excitation within the FE portion of the formulation [16, 17] or impressed electric fields (possibly in form of discrete ports) can be employed, when the driven field problem is solved. As observables, electric fields at individual locations or any kind of integral measure can be monitored in order to find the appropriate pair of $(\omega, \mathbf{k}_{t00})$, i.e., the eigenvalue. For an efficient solution procedure, search algorithms, such as bisection methods in 1D, together with start vector estimation from previous solutions within the employed iterative linear equation solver are used.

5. NUMERICAL RESULTS

The first investigated example is a metallic rectangular hollow waveguide with dielectric-filled corrugations, which has already been considered in [5, 24] with alternative methods and in [13, 15] with similar methods as discussed in this paper, where, however, different aspects have been investigated. A tetrahedral mesh of the unit cell of this 1D periodic configuration is depicted in Fig. 4. The dispersion

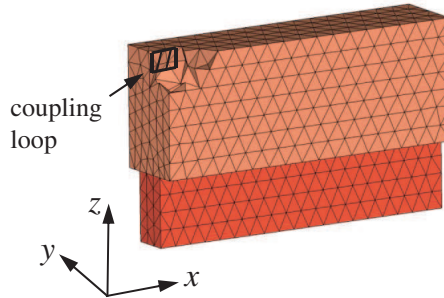


Figure 4. Tetrahedral mesh of computational unit cell of metallic rectangular waveguide with dielectric-filled corrugations according to [24] (see e.g., Fig. 1 in [24]). The tetrahedra in the upper part of the mesh represent the air region in the hollow waveguide, whereas the darker tetrahedra in the lower part represent the dielectric corrugation. Propagation is in y -direction.

characteristic of this unit cell was first computed with the hybrid FEBI method described in Section 4, where only the FE portion was needed for this closed configuration. The excitation of the FE model was realized as a little metallic loop with impressed current and a generator resistance, as indicated in Fig. 4. The average CPU (central processing unit) time required for one excitation solution was about 8sec on a standard PC (personal computer). The obtained dispersion curve is shown in Fig. 5 and compared to reference data from [5] and [24] (scattering matrix approach (SMA)). The agreement of the various curves is very good, where the reference values from [24] are only available in the left-handed band below about 7.6 GHz. The SMA approach in [5] as well as the proposed FEBI method can both deliver the attenuation constant in the bandgap-region from about 7.6 GHz to 8.7 GHz of the waveguide. In the FEBI method, the attenuation constant can be found by a 1D search in this case, since the phase constant is zero in the bandgap. Figs. 6 and 7 show S -parameter resonance curves obtained by CST MWS [18]. In case of Fig. 6, two discrete ports with port resistors of 5000Ω were located very close to each other in the corrugation as indicated in the inset of Fig. 6. Increasing the distance d of the ports from the bottom of the corrugation shows an increasing interaction of the wire ports with the fields causing some change of the resonance behavior. The curves in Fig. 7 were computed with a pair of little wire loop ports with port resistors of 50Ω as indicated in the inset of Fig. 7. Here the influence of the wire ports on the resonance frequency is less, but the width of

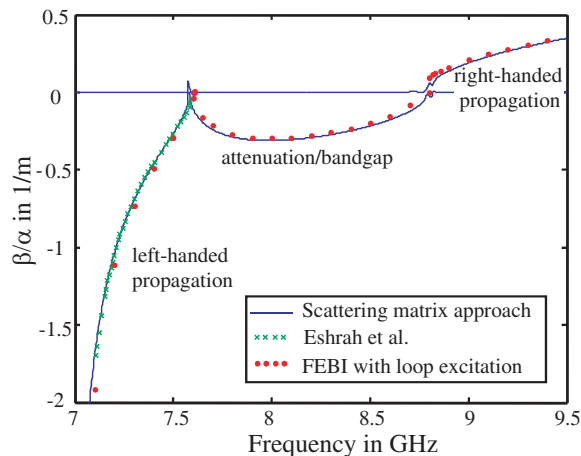


Figure 5. Dispersion diagram of dielectric-filled waveguide as shown in Fig. 4.

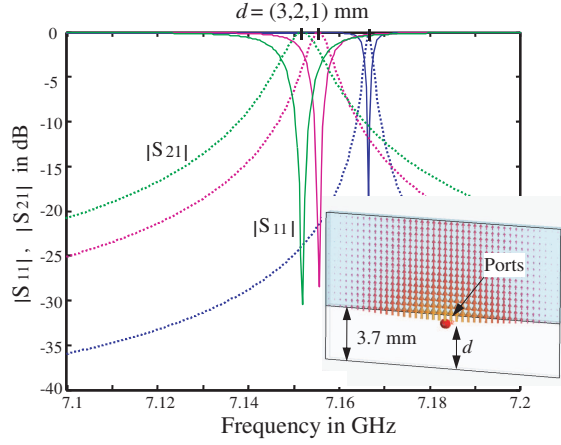


Figure 6. Typical resonance curves computed by CST MWS [18] with respect to the two ports in the corrugation of the unit cell as shown in Fig. 4.

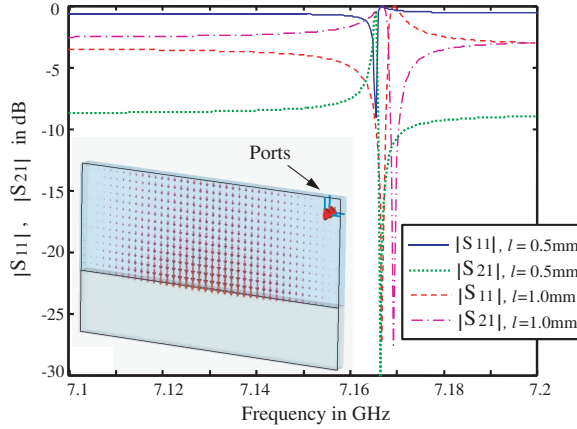


Figure 7. Typical resonance curves computed by CST MWS [18] with respect to the two ports with diameter l in the upper corner (loop excitation) of the unit cell as shown in Fig. 4.

the resonance curve for the 1 mm loop is larger due to the larger input impedance level of a larger loop. From the shape of the resonance curves with loop excitation it is clearly seen that this kind of coupling is not *symmetric* and that additional reactive elements are present due to the coupling. For both excitation types, the port resistors were chosen in order to achieve a reasonable quality factor of the observed

resonance for the given port resistance level.

In the next problem, the 2nd order TE leaky modes (TE_3) with real propagation constant on a grounded dielectric slab of infinite extent are investigated. The slab geometry is depicted in Fig. 8 together with the tetrahedral FE mesh of the chosen doubly periodic unit cell, comprising 9849 tetrahedra. Again, the FEBI method from Section 4 was employed for the analysis, where however the Green's function with Floquet mode series ranging from -1 to $+1$ in both dimensions was modified in a way that it supports the improper leaky substrate modes instead of the proper substrate modes with physical relevance (see e.g., [25] for further information on the leaky substrate modes). Since the dielectric slab is a homogenous waveguide, the FEBI unit cell can be chosen arbitrarily as long as the period is short enough to resolve the wavelength of interest. The excitation of the unit cell was achieved by impressed volume currents within some tetrahedra of the FE portion of the model and the electric field in one observation point was monitored. Some typical resonance curves are shown in Fig. 9 corresponding to TE_3 leaky modes with real propagation constant, which can exist in some frequency range just below the cut-off frequency of the propagating proper TE_3 mode. For the curve labelled with "1 mode becomes propagating", the frequency is set to 25.8 GHz just below the cut-off frequency of the proper TE_3 mode and the leaky mode is moving out of the diagram at the left-hand side to become a proper propagating mode. Another leaky mode is however observed at around $1.2k_0$. For decreasing excitation frequencies (25.6 GHz and 25.4 GHz), two leaky modes with real propagation constant can exist until at a certain frequency (25.2 GHz) no leaky mode with real propagation constant can exist anymore. For these low frequencies the

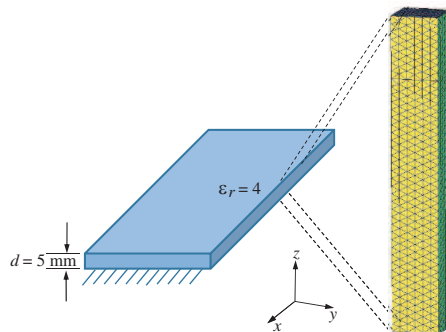


Figure 8. Grounded dielectric slab together with tetrahedral mesh of periodic unit cell.

modes require some attenuation, too. For all considered frequencies, the obtained resonances agree very well with the analytical solutions also shown in Fig. 9. The analytical solutions were found by solving the corresponding transcendental equations (e.g., see [25]). The typical CPU time for the numerical FEBI solution for one excitation was about 2 to 3 sec for this problem.

The next configuration is a composite right/left-handed leaky wave antenna based on a substrate integrated waveguide with interdigital series capacitors as discussed in [26]. The corresponding unit cell is displayed in Fig. 10. The dispersion characteristic of this unit cell as given in Fig. 11 has been determined by computing the corresponding driven problems with the frequency domain tetrahedral solver of CST MWS. Two discrete ports have been used to connect the top and bottom metallizations of the unit cell and the field distribution

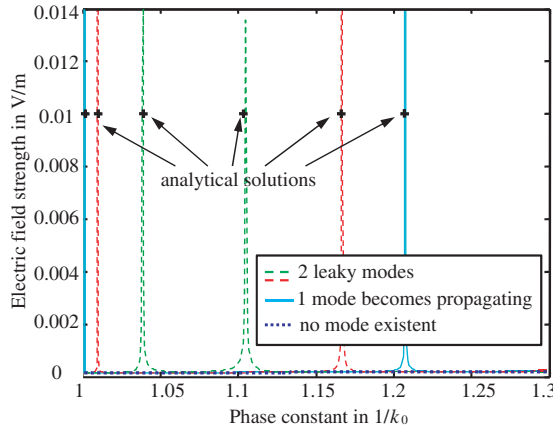


Figure 9. Typical resonance curves of TE_3 leaky modes with real propagation constant for the dielectric slab in Fig. 8. The plus signs indicate the corresponding solutions of the transcendental equations pertaining to the analytical modal field equations (see [25]).

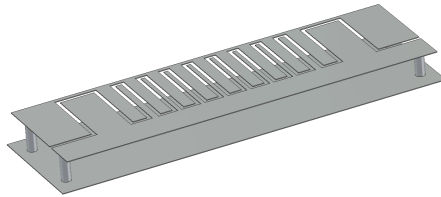


Figure 10. Unit cell of leaky wave antenna according to [26].

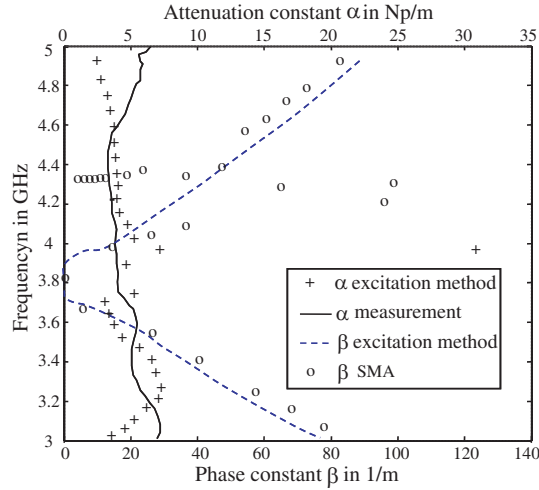


Figure 11. Dispersion diagram and attenuation of unit cell according to Fig. 10 and comparison with scattering matrix approach (SMA) as well as measurement data from [5].

in the guide was monitored in order to detect the resonances. The agreement with the results from the scattering matrix approach in [5] is good. The artefact in the SMA data is due to ill-conditioning of the problem near to the cut-off frequency of the expansion modes [5]. Once the resonances were found, the perturbation method as described in Section 3 was employed in order to compute the attenuation constant as also shown in Fig. 11. The agreement with results obtained from measurements of a fabricated prototype of the antenna is very good, except near the balanced frequency. Careful analysis reveals a small bandgap in the dispersion diagram around 3.8 GHz, where the perturbation method is no longer applicable and must fail. A more detailed discussion of this example and the results is found in [14].

The final problem is a 1D periodic corrugated grounded dielectric waveguide with a unit cell as shown in Fig. 12, which is operated in TE mode and which has also been analyzed in [27] with an SMA and with the matrix pencil method based on the electric field distribution computed by CST MWS for a waveguide of finite length and with waveguide port excitation. The FEBI method from Section 4 was employed for the dispersion analysis of this configuration, where one Floquet mode has been chosen in x - and a series from -19 to $+19$ in y -direction. The utilized tetrahedral FE-mesh comprised 37360 unknowns and the computation time for one excitation was around

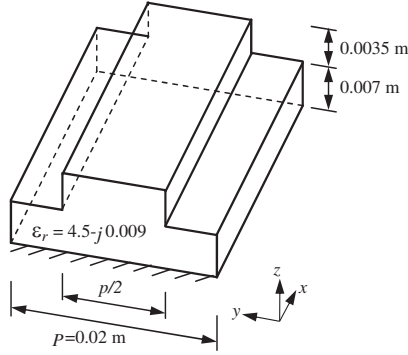


Figure 12. 1D periodic unit cell of grounded corrugated dielectric waveguide (infinite in x) as also considered in [27].

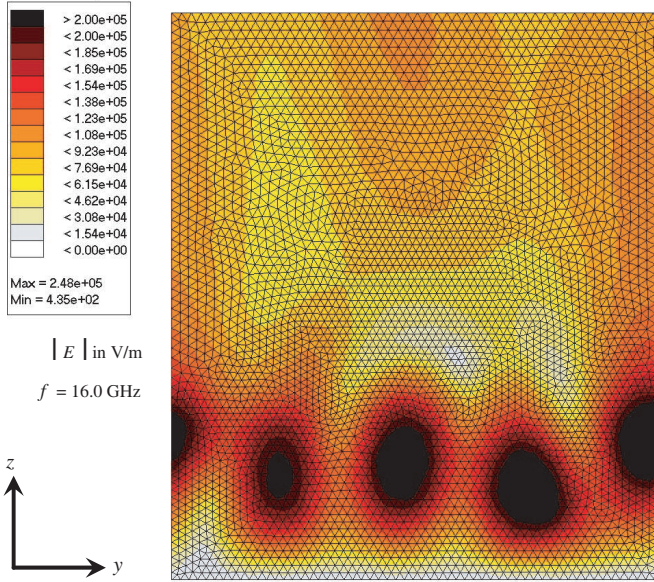


Figure 13. Modal electric field distribution in unit cell according to Fig. 12.

10sec. An impression of the employed tetrahedral mesh is given in Fig. 13, where the computed modal electric field is illustrated in a cut plane through the unit cell for a frequency of 16 GHz. The complex propagation constant $k_{y0} = \beta - j\alpha$ has been directly searched with the FEBI code for every considered frequency, where the sum of the

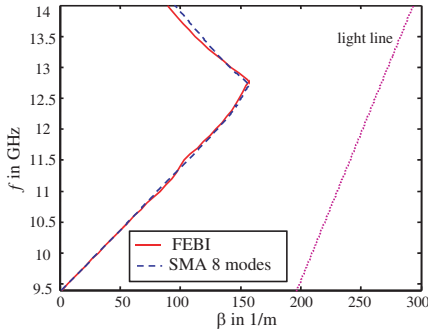


Figure 14. Dispersion diagram of unit cell according to Fig. 12 and comparison with data computed by the scattering matrix approach (SMA) as discussed in [27].

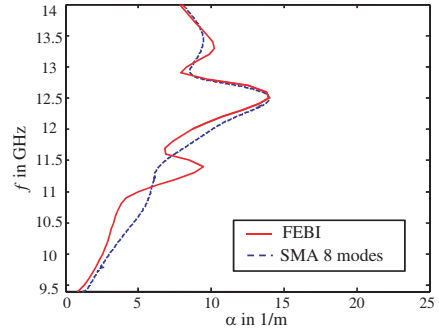


Figure 15. Attenuation constant of unit cell according to Fig. 12 and comparison with data computed by the SMA as discussed in [27].

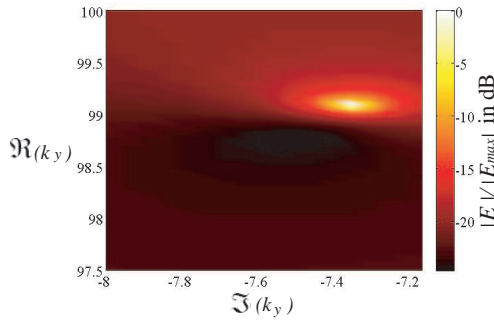


Figure 16. Magnitude of electric field at some observation points within the unit cell according to Fig. 12 for a frequency of 11.4 GHz dependent on the complex wavenumber k_y .

electric field in several observation points within the dielectric was chosen as observable to monitor the resonance behavior. The results for the propagation constant are given in Fig. 14 and for the attenuation constant in Fig. 15. They are compared with SMA results according to the approach discussed in [27], where 8 modes in the SMA have been used and where the absorber was placed 110.5 mm above the ground plane. The observed agreement is very good. An impression of the resonance behavior of the observable is given in Fig. 16. It should be noted that the resonance peak is very sharp and was thus clipped in the illustration.

6. CONCLUSION

Eigenproblem solutions were derived from the resonance behavior of the corresponding excitation problems. In particular, periodic dispersion problems were considered. The field problems are either excited by arbitrary source distributions in the solution domain or by appropriately chosen ports. The eigenvalues are found by monitoring field quantities in the solution domain or the port S -parameters. Together with appropriately implemented periodic boundary conditions, the procedure can directly deliver propagation and attenuation constants. If attenuating periodic boundary conditions are not available or not desirable, small attenuation constants of propagating modes can be determined by perturbation techniques.

The presented results show that the method is accurate and robust, usually even without any regularization. If desired, port resistors or other losses can be used to regularize the typically singular resonance problems, where the port losses can, however, be eliminated from the overall losses in the problem.

ACKNOWLEDGMENT

The authors thank “Deutsche Forschungsgemeinschaft (DFG)” for support of this work under grant EI 352/11-1 and through the TUM International Graduate School of Science and Engineering (IGSSE).

REFERENCES

1. Saad, Y., *Numerical Methods for Large Eigenvalue Problems*, Halstead Press, New York, 1992.
2. Jin, J., *The Finite Element Method in Electromagnetics*, John Wiley & Sons, New York, 2002.
3. Lehoucq, R., D. Sorensen, and C. Yang, *ARPACK Users' Guide: Solution of Large Scale Eigenvalue Problems with Implicitly Restarted Arnoldi Methods*, 1997, <http://www.caam.rice.edu/software/ARPACK/>.
4. Lubkowski, G., B. Bandlow, R. Schuhmann, and T. Weiland, “Effective modeling of double negative metamaterial macrostructures,” *IEEE Trans. Microw. Theory Tech.*, Vol. 57, No. 5, 1136–1146, May 2009.

5. Weitsch, Y. and T. F. Eibert, "Periodically loaded waveguide analysis by evanescent mode superposition," *European Microw. Conf. (EuMC)*, Rome, Italy, 2009.
6. Glock, H.-W., K. Rothmund, M. Borecky, and U. van Rienen, "Calculation of RF eigenmodes using S -parameters of resonator parts," *Proc. EPAC*, 1378–1380, Vienna, Austria, 2000.
7. Kamiya, N. and S. T. Wu, "Generalized eigenvalue formulation of the Helmholtz equation by the Trefftz method," *Engineering Computations*, Vol. 11, 177–186, 1994.
8. Li, Z.-C., "Error analysis of the Trefftz method for solving Laplace's eigenvalue problems," *J. Computational and Applied Mathematics*, Vol. 200, 231–254, 2007.
9. Karageorghis, A., "The method of fundamental solutions for the calculation of the eigenvalues of the Helmholtz equation," *Applied Mathematics Letters*, Vol. 14, 837–842, 2001.
10. Fan, C.-M., D.-L. Young, and C.-L. Chiu, "Method of fundamental solutions with external source for the eigenfrequencies of waveguides," *J. Marine Science and Technology*, Vol. 17, No. 3, 164–172, 2009.
11. Reutskiy, S., "The methods of external excitation for analysis of arbitrarily-shaped hollow conducting waveguides," *Progress In Electromagnetics Research*, Vol. 82, 203–226, 2008.
12. Reutskiy, S. Y., "The method of external excitation for solving generalized Sturm-Liouville problems," *J. Computational and Applied Mathematics*, Vol. 233, 2374–2386, 2010.
13. Eibert, T. F., Y. Weitsch, and H. Chen, "Dispersion analysis of periodic structures by solving corresponding excitation problems," *German Microw. Conf. (GeMiC)*, Darmstadt, Germany, 2011.
14. Chen, H., C. H. Schmidt, T. F. Eibert, and W. Che, "Dispersion and attenuation analysis of substrate integrated waveguides by driven eigenproblem computation," *European Conf. Antennas Propag. (EuCAP)*, Rome, Italy, 2011.
15. Weitsch, Y., H. Chen, and T. F. Eibert, "Dispersion analysis of periodic structures by solving corresponding excitation problems," *Frequenz*, Vol. 65, Nos. 7–8, 247–252, 2011.
16. Eibert, T. F., J. L. Volakis, D. R. Wilton, and D. R. Jackson, "Hybrid FE/BI modeling of 3D doubly periodic structures utilizing triangular prismatic elements and a MPIE formulation accelerated by the Ewald transformation," *IEEE Trans. Antennas Propag.*, Vol. 47, No. 5, 843–850, May 1999.

17. Eibert, T. F., Y. E. Erdemli, and J. L. Volakis, "Hybrid finite element-fast spectral domain multilayer boundary integral modeling of doubly periodic structures," *IEEE Trans. Antennas Propag.*, Vol. 51, No. 9, 2517–2520, Sept. 2003.
18. CST Microwave Studio, 2010, <http://www.cst.com>.
19. Bondeson, A., T. Rylander, and P. Ingelstrom, *Computational Electromagnetics*, Springer Science, New York, 2005.
20. Davidson, D. B., *Computational Electromagnetics for RF and Microwave Engineering*, 2nd edition, Cambridge University Press, Cambridge, UK, 2011.
21. Baum, C. E., E. J. Rothwell, K.-M. Chen, and D. P. Nyquist, "The singularity expansion method and its application to target identification," *Proc. IEEE*, Vol. 79, No. 10, 1481–1492, 1991.
22. Kong, J. A., *Electromagnetic Wave Theory*, 2nd edition, Wiley Interscience, New York, USA, 2009.
23. Tamir, T. and A. A. Oliner, "Guided complex waves. Part 1: Fields at an interface," *Proc. IEE*, Vol. 110, No. 2, 310–324, Feb. 1963.
24. Eshra, I. and A. Kishk, "Analysis of left-handed rectangular waveguides with dielectric-filled corrugations using the asymptotic corrugation boundary," *IEE Proc. Microw. Antennas Propag.*, Vol. 153, No. 3, 221–225, Jun. 2006.
25. Hsu, C., R. Harrington, J. Mautz, and T. Sarkar, "On the location of leaky wave poles for a grounded dielectric slab," *IEEE Trans. Microw. Theory Tech.*, Vol. 39, No. 2, 346–349, Feb. 1991.
26. Weitsch, Y. and T. F. Eibert, "Composite right-/left-handed interdigital leaky-wave antenna on a substrate integrated waveguide," *European Conf. Antennas Propag. (EuCAP)*, Barcelona, Spain, 2010.
27. Weitsch, Y. and T. F. Eibert, "Eigenvalue computation of open periodically composed waveguides by series expansion," *IEEE Antennas Propag. Soc. Int. Symp.*, Spokane, WA, Jul. 2011.